Express Polymer Letters Vol.16, No.1 (2022) 75–84
Available online at www.expresspolymlett.com
https://doi.org/10.3144/expresspolymlett.2022.6

Research article

Synthesis of linear poly-cardanol and its application in rubber materials

Wei Qian[1], *Jinling Liu*[2], *Yuxia Zhang*[1], *Chongyi Chi*[1], *Denglong Chen*[2], *Qinhui Chen*[1*]

[1]College of Chemistry and Materials Science, Fujian Normal University, Fuzhou, 350007 Fujian, P R China
[2]Quangang Petrochemical Research Institute of Fujian Normal University, Quanzhou, 362800 Fujian, P R China

Received 11 June 2021; accepted in revised form 19 August 2021

Abstract. People have been trying to find natural products that can replace rubber due to the land occupied by rubber planting and the environmental pollution caused by waste rubber. Herein, the linear poly-cardanol (LPCA) is obtained by undergoing a Friedel-Crafts alkylation reaction at 100 °C for 2 h at the catalyst of 5% of p-toluene sulfonate. The M_w of LPCA is about $4 \cdot 10^4$, and its polymeric degree is about 133. The weakening of 3009, 1263, and 1154 cm^{-1} in IR spectrum, the blue shift of UV absorption, the new chemical shifts of protons in ^{1}H-NMR spectrum all certify the formation of LPCA. LPCA has obvious characteristics of elastomer. Its glass transition temperature (T_g) is –20.7 °C on the DSC curve. During the co-crosslinking of LPCA and liquid polyisoprene rubber (LIR), LPCA induces the crystallization of long LIR chain segments, which is confirmed by the transition peaks of the DSC curve in 40 °C. This partial crystal structure is beneficial for LPCA/LIR blends to possess high strength. The tensile strength and the elongation at break of LPCA/LIR blend with 20% of LIR are about 2.04 MPa and 92%, respectively. LPCA possesses flexible alkyl chains and hydrophilic phenolic hydroxyl groups, so it can be used as a plasticizer just like LIR and compatibilizer at the same time. This study affords a possible way for renewable cardanol to replace rubber partially or completely.

Keywords: *polymer blends and alloys, cardanol, Friedel-Crafts reaction, rubber, crystallization*

1. Introduction

Wheels change the world. The rapid development of society and economy can be inextricably linked to the contribution of the rubber industry [1, 2], which is widely used in industry [3], agriculture [4], medical, and health applications [5, 6]. Rubber is derived from rubber trees and petroleum-based synthetic materials mainly. The large-scale planting of rubber trees leads to the irreversible destruction of tropical rain forests and the consequent ecological and environmental problems [7]. The increasing consumption of petroleum-based resources [8] exacerbates the energy crisis. In addition, a large number of wastes from the rubber industry, as discarded tires [9–11], sealing caps [12, 13], soles [14], *etc*., brought great challenges to environmental protection, human health, and economic development [15]. It is difficult for these waste rubber with covalent crosslinking three-dimensional network structures to be degraded. According to reports [16], about 1 billion tires and many sealing caps are abandoned every year, and nearly half of them are buried and incinerated [17]. Both landfill and incineration result in environmental pollution, ecological harm, the scarcity of rubber resources, and many lands occupied. Therefore, renewable elastomer that can replace or partially replace rubber is urgent.

Cardanol (CA), a vegetable oil refined from waste cashew nutshell, is a green, environmentally friendly, and renewable industrial raw material (Figure 1). It is a phenolic compound with a certain polarity and unbranched saturated carbon chains or olefins composed

*Corresponding author, e-mail: chenqh@fjnu.edu.cn

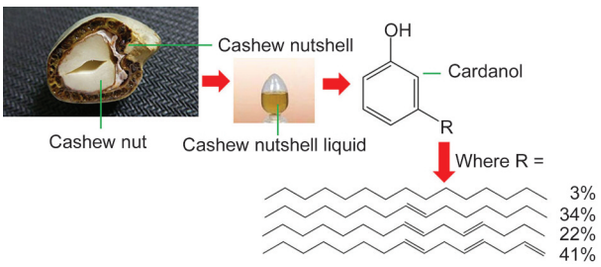

Figure 1. Origination and chemical structure of cardanol.

of 15 carbons in the meta-position. Among them, saturated carbon chain, monoene, diene, and triene account for 3, 34, 22, and 41%, respectively [18]. This provides the possibility for its addition reaction, esterification, nitration, *etc*. Cardanol with abundant sources, low price, and excellent performance attracts the attention of researchers. There are many modified products, such as cardanol phenolic resin, cardanol-based epoxy resin, cardanol-based surfactants, polyepoxy-cardanol glycidyl ether, and so on, which are widely used in toughening [19–21], flame retardant [22], coating [23], adhesive [24, 25], curing agents [26] and many other industrial fields. This attracts researchers' attention to study cardanol potential applications in the rubber industry [27].

Dhanania *et al.* [28] grafted phosphorylated cardanol prepolymer (PCP) onto guayule natural rubber (GNR) by solution polymerization. The maximum grafting rate and the grafting efficiency were 6.1 and 84.7%, respectively. Compared with GNR, the T_g of PCP-*g*-GNR is slightly lower due to the introduction of PCP. Prabhavale *et al.* [29] grafted PCP onto the main chain of carboxylated styrene-butadiene rubber (XSBR) by the melt grafting method. Then PCP-*g*-XSBR is mixed with silica particles. The filler is well dispersed in PCP-*g*-XSBR, so the product showed excellent mechanical properties as Mooney viscosity and plasticity number. The optimum curing time of PCP-*g*-XSBR decreased by 8, 8, and 37 s, respectively, compared with XSBR. In addition, the vulcanized PCP-*g*-XSBR has good thermal stability. Samantarai *et al*. [30] studied the grafting of cardanol onto carboxylated acrylonitrile-butadiene rubber (XNBR) by emulsion polymerization. Compared with XNBR, XNBR grafted by cardanol showed lower T_g, Mooney viscosity, plasticity number (higher plasticity) and damping value, higher thermal stability, curing rate, and plasticity retention index. Samantarai *et al*. [30] also studied the grafting of CA and PCP with acrylonitrile butadiene rubber (NBR), respectively. Both CA-*g*-NB [31] and PCP-*g*-NBR [32] showed lower glass transition temperature, enhanced plasticization compared to NBR. These offer better processability and technical properties. Mohapatra *et al*. investigated the chemical grafting of cardanol with natural rubber at the latex stage (CGNR) [33]. The higher molecular weight and lower meniscus viscosity of CGNR compared to NR indicated its plasticizing effect [34]. Further studies showed that the phenolic hydroxyl groups of cardanol interact with siloxanes and silane functional groups, which enhances the interaction between rubber and filler, and exhibits very good compatibilization [35]. Zhang *et al*. [36] obtained chloroprene rubber (CR) covalently bonded with cardanol by click chemistry, which overcame the migration of plasticizers and improved the processing performance of rubber.

The low grafting rate hinders cardanol from being used in the rubber industry in quantity. It is a feasible method for rubber to co-crosslink with preplymerized cardanol to heighten the usage of cardanol in the rubber industrial (Figure 2). Herein, the linear polymerized cardanol (LPCA) was synthesized by

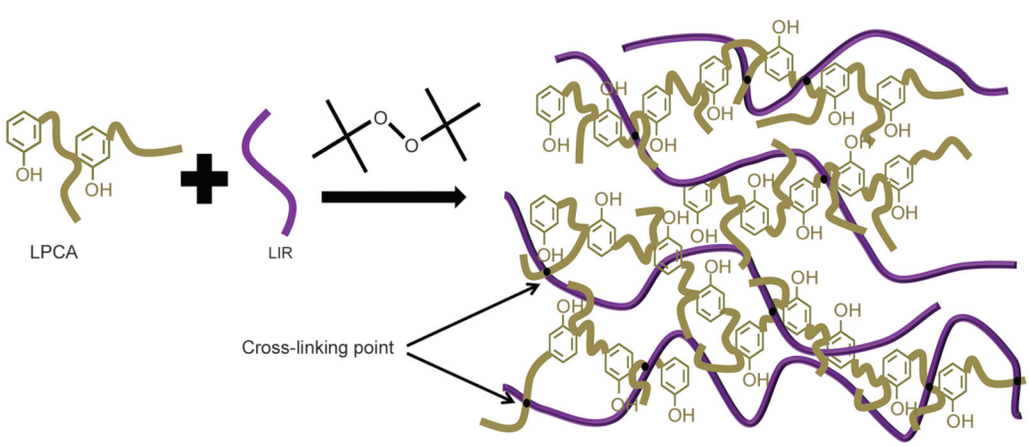

Figure 2. Schematic diagram of co-crosslinking between LPCA and LIR.

the Friedel-Crafts alkylation reaction CA in the absence of solvent. It is easier for LPCA with lengthened hydrophobic carbon chains to crosslink with LIR than CA because of their increased compatibility. The molecular structure and polymerized mechanism of the obtained LPCA were characterized by viscosity, gel permeation chromatography (GPC), Fourier transform infrared (FTIR) analysis, nuclear magnetic resonance (NMR), and ultraviolet spectroscopy (UV). Then the mechanical properties and the thermal stability of LPCA/LIR blends were discussed. LPCA originated from renewable cardanol in solvent-free conditions is a green product. It is a potential material to replace rubber partially or all.

2. Experimental

2.1. Materials

Cardanol was purchased from Fujian Jianyang Xinhua Chemical Co. Ltd. Liquid polyisoprene rubber (molecular weight 30 000) was purchased from Shenzhen Masini Elastomer Co., Ltd. Petroleum ether, anhydrous ethanol, p-toluene sulfonate monohydrate, Di-t-butyl peroxide (DTBP), isocyanuric acid triallyl ester (TAIC), Tetrahydrofuran (THF), dimethylbenzene, deuterated chloroform were purchased from Sinopharma Chemical Reagents Co. Ltd.

2.2. Preparation of linear polymerized cardanol (LPCA)

3, 5, 7, and 9% of p-toluene sulfonate as protic acid was added into a reactor contained 300 g of cardanol. The reactor was stirred at different temperatures of 70, 80, 90, and 100 at 300 r/min for a certain period. Then the stirring is stopped, and the reactor was maintained in an oil pot for 2 h to obtain LPCA with high molecular weight.

2.3. Preparation of LPCA/LIR blends

A certain ratio of LPCA, LIR, vulcanizing agent, and its co-agent (Table 1) was added into a reactor and mixed at 70 °C for 3 hours. Then, the mixture was poured into a preheated mold and cured at the temperature of 120 and 140 °C for 2 hours, respectively. After cooled to room temperature, the LPCA/LIR blends were prepared.

Table 1. Formulation of LPCA/LIR blends.

Sample	10:0	9:1	8:2	7:3
LPCA	100	90	80	70
LIR	0	10	20	30
DTBP	0.2	0.2	0.2	0.2
TAIC	0.2	0.2	0.2	0.2

2.4. Testing and instruments

2.4.1. Ultraviolet spectrum

The ultraviolet spectra of cardanol and LPCA were recorded in an ultraviolet spectrophotometer (TU-1901, Beijing Pullout General Instrument Co. Ltd., China) at the wavelength range of 200–325 nm, at the scanning frequency of 0.5 nm/s and ethanol used as the solvent.

2.4.2. Infrared spectrum

Fourier transform infrared spectrometer (Nicolet 5700, Thermo, USA) was used to obtain the IR spectra of CA and LPCA by ATR method at a resolution of 2 cm^{-1} and a scanning range of 600~4000 cm^{-1}.

2.4.3. Viscosity measurement

The viscosity of LPCA was measured in a rotary rheometer (3-NDJ-8S, Shanghai Yueping, China) at the temperature of 70 °C and the result was read in 30 s.

2.4.4. Molecular weight and its distribution

Gel permeation chromatography (WATERS 1515, USA) was selected to decide the molecular weight and the distribution of LPCA. The flow rate of tetrahydrofuran was 1.0 ml/min, and the injection volume was 100 ul.

2.4.5. ^{1}H-NMR measurement

^{1}H-NMR spectra of cardanol and LPCA were determined by AVANCE II 400 NMR spectrometer (Bruker, Switzerland) at room temperature and $CDCl_3$ as solvent.

2.4.6. SEM measurement

The cross-section of LPCA/LIR blends was observed by cold-field scanning electron microscopy (SEM, JEOL-7500LV, JEOL Ltd., Japan) after the samples were vacuum-sputtered with gold at an accelerating voltage of 5 kV and a current of 20 μA.

2.4.7. Tensile test

The mechanical properties of blends were analyzed by universal testing machine (LLOYD LR5Kplus, UK) according to GB/T 1040.1 test standards. The tensile rate is 50 mm/min, and 7 samples of each group are measured. The outlier values were abandoned

according to the Grubbs method. Then the average value and the average deviation were obtained.

2.4.8. DSC measurement

The thermal properties of the blends were investigated by differential scanning calorimetry (DSC3, Mettler, Switzerland) at a heating rate of 5 °C/min from –80 to 80 °C.

2.4.9. DMA measurement

Dynamic mechanical analysis (DMA, Mettler-Toledo DMA1, Swiss) was carried out at a heating rate of 5 °C/min from –80 to 80 °C and a frequency of 1 Hz.

3. Results and discussion

3.1. Origination and structure of LPCA

97% of cardanol possesses one or more double bonds, so it is possible for cardanol to react between double bonds of the long side chain and the active hydrogen of the benzene ring in the presence of protic acid. That is to say; there is a Friedel-Crafts alkylation reaction between the ortho or para position of phenol groups and the double bonds of the other cardanol molecule. The specific process is shown in Figure 3. The double bond on the unsaturated side chain of cardanol is electrophilically added by H^+ of protic acid, resulting in the formation of a carbocation. The carbocation attaches the ortho or para position of cardanol phenol groups, thus generating dimer. The process is repeated, and macromolecular LPCA is formed.

It is obvious that the molecular chains increase with the reactive time prolonged. As a result, a gel status Bingham fluid generates. Figure 4a shows the effects of catalyst dosage and reactive temperature on the formation time of Bingham fluid. For the same temperature, the gelation time decreases with the increase of the amount of catalyst, which is attributed

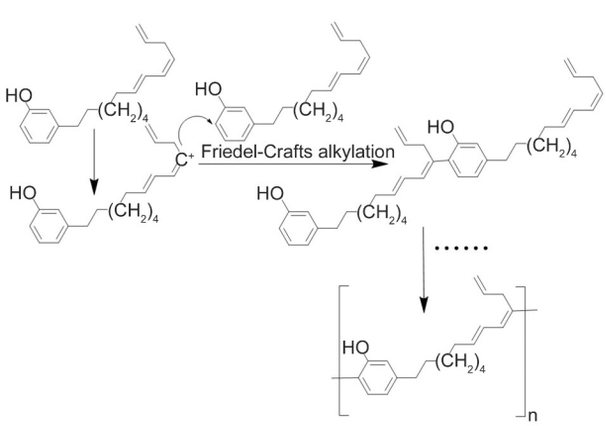

Figure 3. Diagram of the polymeric mechanism of LPCA.

to the increase of the concentration of free radicals. The effect of reactive temperature on gelation time is similar to the catalyst dosage because high temperature affords more energy for the activation of a catalyst than low temperature. It is necessary for the gelation of cardanol to use 9% catalyst at 70 °C. Otherwise, it is impossible to obtain gelation Bingham fluid. In this paper, the polymerization is carried out at a temperature of 100 °C in the presence of 5% of p-toluene sulfonic acid monohydrate. Figure 4b shows the molecular weight and the distribution of LPCA after cardanol polymerized for two hours. The molecular weight (M_w) of LPCA is $4 \cdot 10^4$, and its dispersity is broad because cardanol is a mixture containing saturated carbon chain, monoene, diene, and triene. The molecular weight of cardanol is 300. The degree of polymerization of cardanol is about 133. The increase of molecular chains increases viscosity. Figure 4c shows the viscosity of LPCA increases with the polymeric time prolonged monotonously till reacted for 6h when the value exceeds the measurement limit. It is inevitable for LPCA to crosslink into a three-dimensional network at excessive viscosity because diffusion becomes very difficult. From Figure 4d and Figure 4e, it can be found that LPCA polymerized for 2 h can be dissolved in petroleum ether and xylene and that for 6 h can't. In order to control the polymeric degree of cardanol, 2 h is selected as reactive time. It is key for the followed co-crosslinking to control polymeric time for good compatibility and adequate unsaturated bonds.

Figure 5a shows the IR spectra of cardanol and LPCA. As can be seen from the spectrum of cardanol, the peak at 3342 cm^{-1} corresponded to the phenolic hydroxyl group, the characteristic stretching vibration of C–H due to the double bonds of the alkyl chain at 3009 cm^{-1}. The peaks at 2926 and 2854 cm^{-1} are due to the asymmetric stretching vibration of methylene and methyl groups in the long aliphatic chain, respectively. The peaks at 1589, 1488, and 1456 cm^{-1} represent the stretching vibration of the benzene ring. 1263, 1154 cm^{-1} are attributed to the symmetric and asymmetric stretching of C=C, respectively. The peaks of 693 cm^{-1} represent the C–H trans-bending vibration of the olefin. Compared with cardanol, the hydroxyl peak of LPCA decreases significantly, which is caused by the oxidation of phenolic hydroxyl groups. The weakening of 3009, 1263, and 1154 cm^{-1} just means that double bonds of the side chain react with the ortho or para

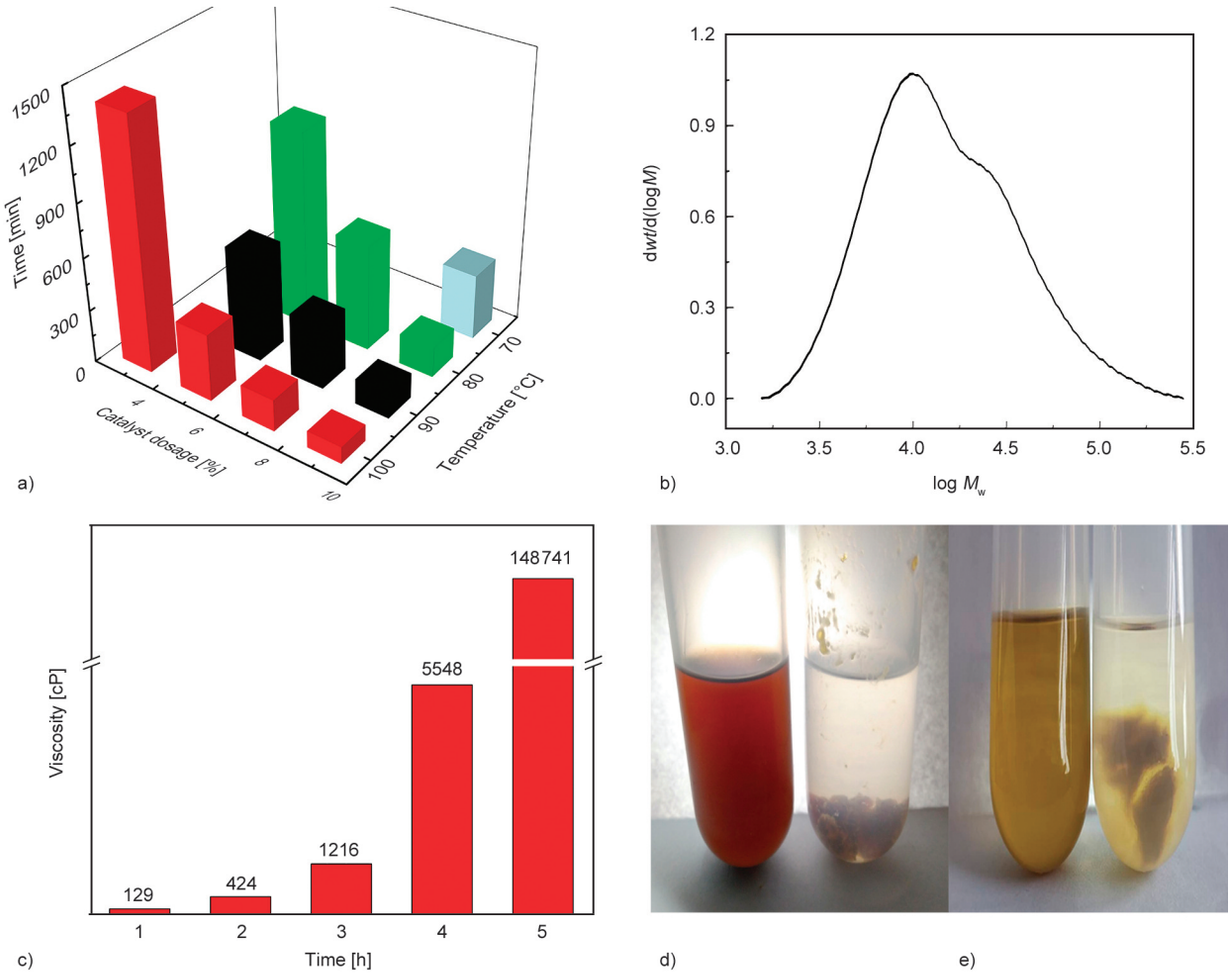

Figure 4. (a) Effects of catalyst dosage and reactive temperature on the formation time of Bingham fluid; (b) GPC spectrum of LPCA when CA polymerized in 100 °C for 2 h in the presence of 5% catalyst; (c) Viscosity *vs*. polymeric time; LPCA obtained by polymerization for 2 h (left) and 6 h (right) dissolved in (d) petroleum ether and (e) xylene.

position of the phenolic group among different cardanol molecules during Friedel-Crafts alkylation.

Cardanol is a derivative of phenol with long side chains with different saturation. It can generate n→π* and π→π* electronic transitions and form absorption bands in the UV spectrum. Figure 5b is the UV spectra of Cardanol and LPCA in anhydrous ethanol. As can be seen from Figure 5b, cardanol has a strong absorption peak at 220 nm, which is the E absorption band of the benzene ring and double bonds. Besides, the B absorption band of the benzene ring appears at 274 nm. However, the E absorption band of LPCA blue shifts by about 6nm. At the same time, the fine structure of B absorption disappears completely. That's because the increase in benzene ring substitution degree increases the electron fluidity between the unsaturated side chain and the aromatic ring. This reason is that the Friedel-Crafts alkylation between double bonds of the unsaturated side chain and the benzene ring increases substitution degree. As a result, the electron fluidity of the unsaturated bonds and the aromatic rings increases. Electronic migration between energy levels becomes difficult because of the increased binding capacity of the nucleus.

Figure 5c and Figure 5d are the ^{1}H-NMR spectra of cardanol and LPCA. The chemical shifts of protons **a** (Ph-C**H**(CH=CHCH$_3$)–), **b** (–C**H$_2$**–C=C-trans), and **c** (=C**H**–CH$_3$) are observed in LPCA, but not in cardanol. The results of ^{1}H-NMR analysis further confirm that LPCA originates from the polymerization among different CA molecules accompanied by the increase of the benzene ring substitution degree. These results are consistent with FTIR and UV, which all indicate that the unsaturated side chain and ortho or para position of phenolic groups in CA react one by one in the presence of p-toluene sulfonic acid.

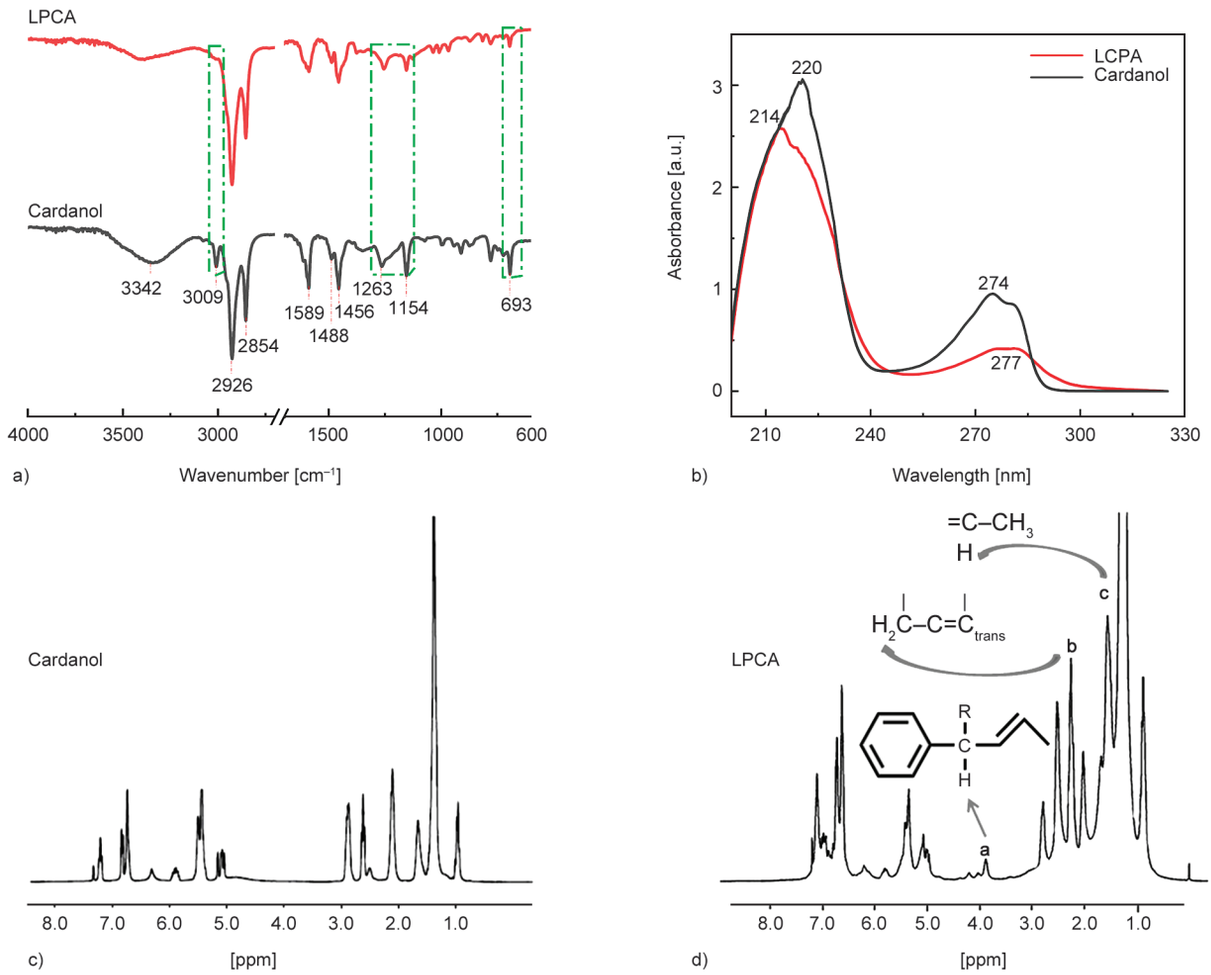

Figure 5. (a) IR (b) UV spectra of CA and LPCA; ^{1}H-NMR spectra of CA (c) and LPCA (d).

3.2. Characteristics of LPCA/LIR blends

Figure 6 is the cross-section SEM images of LPCA/LIR blends after being heat cured. It can be seen from Figure 6a shows that there are lots of crazes in the direction perpendicular to the striped crack. Meanwhile, these striped cracks are long and deep, accompanied by branching. These factors are beneficial for LPCA to dissipate a lot of energy. When 10% of LIR is added into LPCA, the LPCA/LIR blends show a typical island-in-sea structure (Figure 6b). The dispersed phase size is about 10 nm. The interfacial adhesion of dispersed LIR phase and LPCA matrix is good, and part of LIR is broken in two. There are many little and shallow dimples, which are distributed at random. With LIR increased to 20%, the LIR dispersion size changes greatly, and the broken LIR can also be clearly observed. Moreover, the larger and deeper dimples than that of 10% LIR extend to one direction (Figure 6c). Once the usage of LIR increased to 30%, the interfacial adhesion does decrease obviously. There is no fractured LIR phase and some LIR phases adjoined with each other on the cross-section. That is to say, the dispersed phase agglomerates (Figure 6d).

The glass transition temperature (T_g) of LPCA/LIR blends is shown in Figure 7. Results show that there is only one transition step at –20.7 °C for LPCA. The low T_g means that LPCA is suitable for elastomer and even replaces rubber. With the addition of LIR, the T_g of LPCA/LIR blends rises first and then lowers. When 10% of LIR is used, LPCA is crosslinked with LIR. The increased crosslinking degree prevents the movement of LPCA chains, so the T_g of LCPA/LIR blends increases. Then, the increased LIR usage forms the LIR microphase. The T_g of LPCA/LIR blends is decided by the T_g of the two phases and their compatibility. The T_g of LIR is –63 °C [37]. The T_g of LPCA/LIR blends should be between –63 and –20.7 °C, so it decreases to –32.1 and –31.4 °C, respectively, when LIR is 20 and 30%. What is more noteworthy is the new transition stage of LPCA/LIR blends at about 36 °C caused by the crystallization

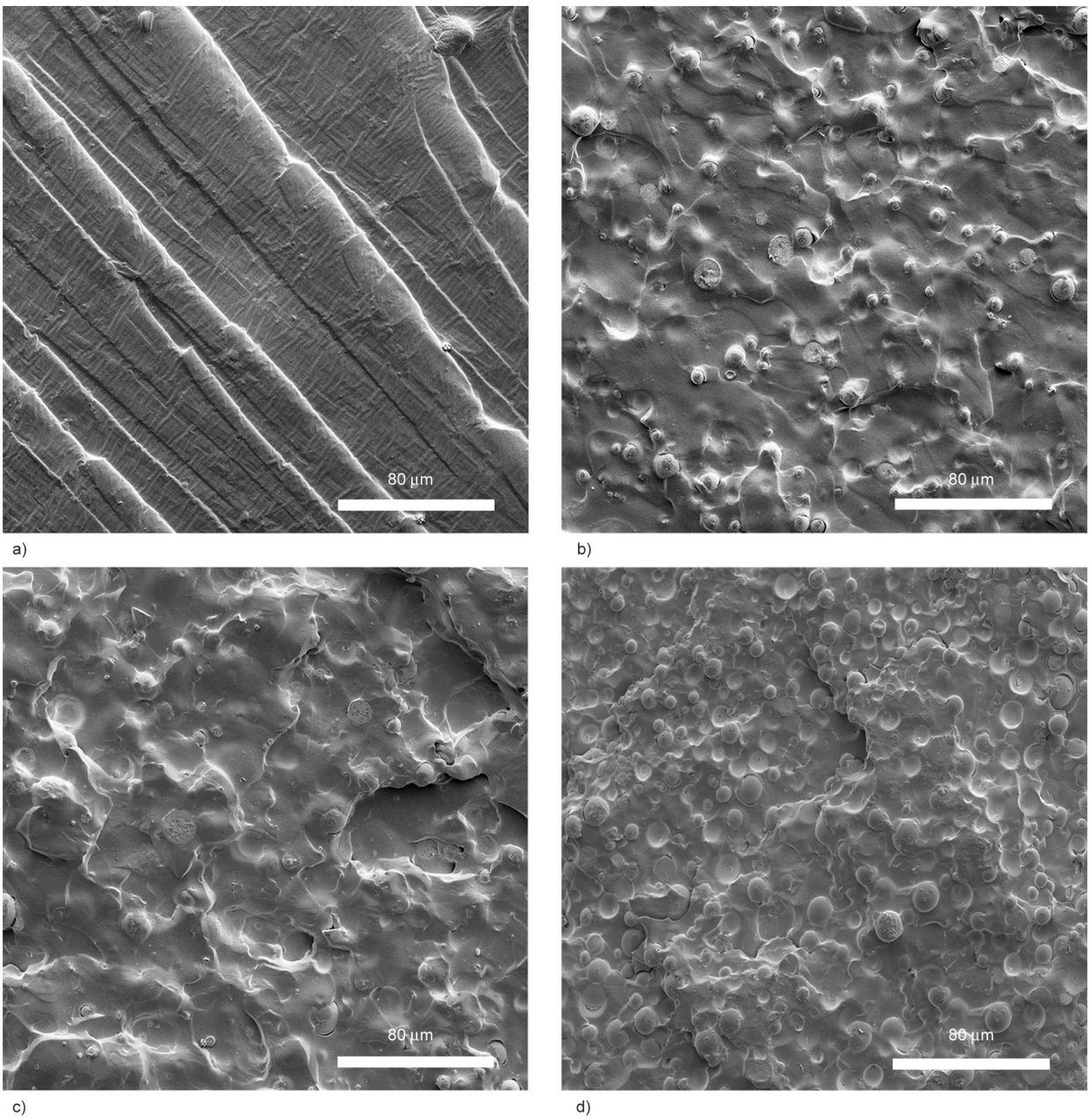

Figure 6. SEM images of LPCA/LIR: (a) 10:0 (b) 9:1 (c) 8: 2 (d) 7: 3.

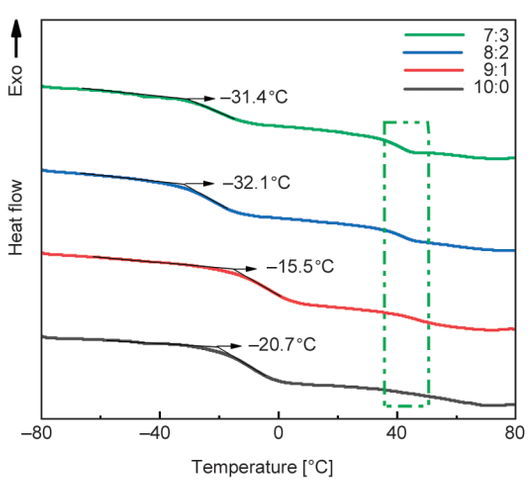

Figure 7. DSC curves of LPCA/LIR blends.

of the long LIR chain segment induced by LPCA [38]. Under the same vulcanizing condition, pure LIR can't be cured completely, so the crystallization of LIR is at the action of LPCA as described in the literature [38]. This crystallization transition is more and more obvious with the increase of LIR.

Figure 8 shows the function of loss coefficient (tan δ) and dynamic storage modulus (E') of LPCA/LIR blends over the temperature range. It can be seen in Figure 8a shows that the dynamic storage modulus of all samples is above 10^9 Pa below T_g. When LPCA/LIR is 9:1, the dynamic storage modulus is slightly higher than that of LPCA between T_g and T_c. This is attributed to the double effects of the rigidity

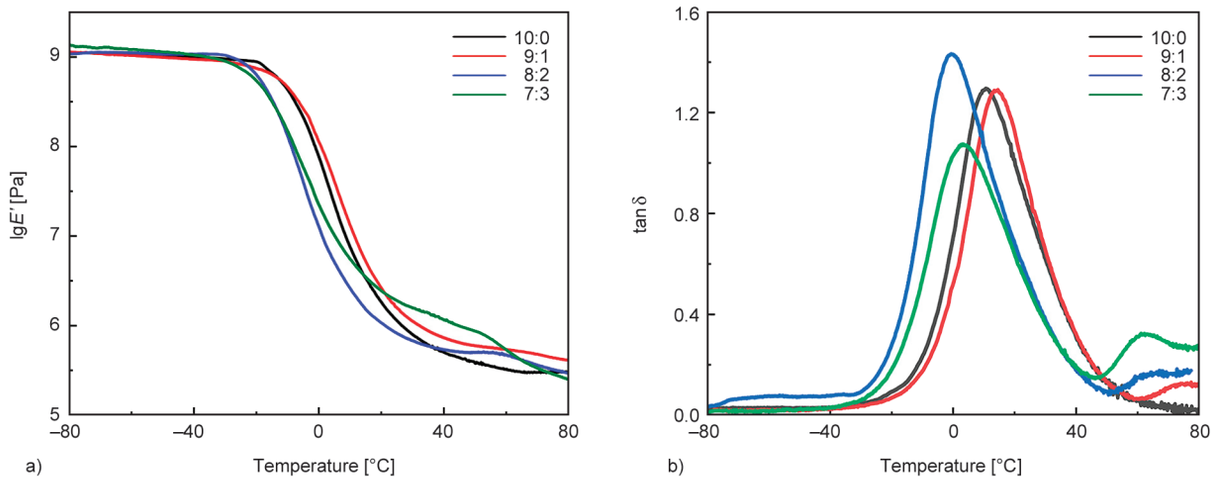

Figure 8. Effect of dynamic storage modulus (E') (a) and loss factor (tan δ) (b) as a function of temperature.

of the benzene ring and the crystallization of the long LIR chain segment induced by LPCA. With the ratio change of LPCA and LIR, these two effects go up and down. The changing trend of tan δ is consistent with that of DSC results. Similarly, the reason is the combined effects of the co-crosslinking between LPCA and LIR, the rigidity of LPCA, and the crystallization of LIR. When LPCA/LIR is 8:2, the loss factor increases dramatically. At the same time, the melting peak of the crystal decreases. The increased amorphous phase and the increased crosslinking degree result in that LPCA/LIR blends show increased viscosity. The damping coefficient of LPCA/LIR (7:3) decreases significantly due to the reduction of the amorphous phase. In other words, the agglomeration of LIR at this time increased its crystallinity.

Figure 9 shows the tensile strength and elongation at break with different LIR content, and the data are summarized in Table 2. Obviously, the tensile strength

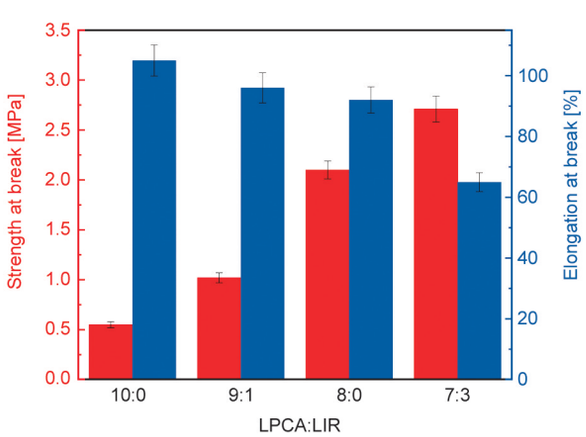

Figure 9. Diagrams of tensile strength and elongation at breaking of LPCA/LIR blends.

Table 2. Mechanical data of LPCA/LIR blends.

LPCA:LIR	Stress [MPa]	Elongation at break [%]
10:0	0.54±0.05	100±7
9:1	1.00±0.10	95±6
8:2	2.04±0.28	92±13
7:3	2.64±0.33	63±10

of LPCA/LIR blends increases with the increase of LIR content because of its crystallization. It can be seen that the elongation at break decreases with the rise of LIR content. The elongation at break decreases slightly when the LIR content is limited to 20% and decreases significantly when the content of LIR is further added because of poor interfacial adhesion. The excessive LIR hinders the alkyl chains entanglement of LPCA.

4. Conclusions

The linear poly-cardanol (LPCA) was obtained by Friedel-Crafts alkylation reaction at 100 °C for 2 h at the catalyst of 5% of p-toluene sulfonate. The M_w of LPCA is about $4 \cdot 10^4$, and its degree of polymerization is about 133. The weakening of 3009, 1263, and 1154 cm^{-1} in the IR spectrum, the blue shift of the UV absorption, the new chemical shifts of protons in ^{1}H-NMR spectrum all certified the formation of LPCA. LPCA has obvious characteristics of elastomer. Its T_g is –20.7 °C in the DSC curve. During the co-crosslinking of LPCA and LIR, LPCA induces the crystallization of the long LIR chain segment, which is confirmed by the transition peaks of the DSC curve at 40 °C. This partial crystal structure is beneficial for LPCA/LIR blends to possess high

strength. The tensile strength and elongation at break of LPCA/LIR blends containing 20% LIR were about 2.04 MPa and 92%, respectively. LPCA possesses flexible alkyl chains and hydrophilic phenolic hydroxyl groups, so it can be used as a plasticizer just like LIR and compatibilizer at the same time. This study affords a possible way for renewable cardanol to replace rubber partially or all.

Acknowledgements

This work was supported by the National Natural Science Foundation of China (No. 51773038) and the Natural Science Foundation of Fujian Province (No. 2020J01150).

References

[1] Woodruff W.: Growth of the rubber industry of Great Britain and the United States. The Journal of Economic History, **15**, 376–391 (2011). https://doi.org/10.1017/s0022050700056540

[2] Syahza A., Backe D., Asmit B.: Natural rubber institutional arrangement in efforts to accelerate rural economic development in the province of Riau. International Journal of Law and Management, **60**, 1509–1521 (2018). https://doi.org/10.1108/ijlma-10-2017-0257

[3] Moreno-Ríos M., Gallardo-Hernandez E. A., Yáñez-Escoto M. J., Márquez-Tamayo L. A., Iturbe-Salas E.: Evaluation of surface modification in a steel track for the rubber tyred metro. Wear, **426**, 1265–1271 (2019). https://doi.org/10.1016/j.wear.2018.12.021

[4] Ansari A. H., Jakarni F. M., Muniandy R., Hassim S., Elahi Z.: Natural rubber as a renewable and sustainable bio-modifier for pavement applications: A review. Journal of Cleaner Production, **289**, 125727 (2021). https://doi.org/10.1016/j.jclepro.2020.125727

[5] Rahimi A., Mashak A.: Review on rubbers in medicine: Natural, silicone and polyurethane rubbers. Plastics, Rubber and Composites, **42**, 223–230 (2013). https://doi.org/10.1179/1743289811y.0000000063

[6] Yu Y., Ye L., Song Y., Guan Y., Zang J.: Wrinkled nitrile rubber films for stretchable and ultra-sensitive respiration sensors. Extreme Mechanics Letters, **11**, 128–136 (2016). https://doi.org/10.1016/j.eml.2016.12.003

[7] Rosa J. R. B. F., Mantello C. C., Garcia D., de Souza L. M., da Silva C. C., Gazaffi R., da Silva C. C., Toledo-Silva G., Cubry P., Garcia A. A. F., de Souza A. P., le Guen V.: QTL detection for growth and latex production in a full-sib rubber tree population cultivated under suboptimal climate conditions. BMC Plant Biology, **18**, 223 (2018). https://doi.org/10.1186/s12870-018-1450-y

[8] Sorrell S., Speirs J., Bentley R., Brandt A., Miller R.: Global oil depletion: A review of the evidence. Energy Policy, **38**, 5290–5295 (2010). https://doi.org/10.1016/j.enpol.2010.04.046

[9] Hamdi A., Abdelaziz G., Farhan K. Z.: Scope of reusing waste shredded tires in concrete and cementitious composite materials: A review. Journal of Building Engineering, **35**, 102014 (2021). https://doi.org/10.1016/j.jobe.2020.102014

[10] Celauro B., Celauro C., Lo Presti D., Bevilacqua A.: Definition of a laboratory optimization protocol for road bitumen improved with recycled tire rubber. Construction and Building Materials, **37**, 562–572 (2012). https://doi.org/10.1016/j.conbuildmat.2012.07.034

[11] Plesuma R., Malers L.: Some functional properties of composite material based on scrap tires. Open Engineering, **3**, 492–498 (2013). https://doi.org/10.2478/s13531-013-0113-x

[12] Wang W., Pang X., Zheng C., Volinsky A. A.: Failure analysis of high nickel alloy steel seal ring used in turbomachinery. Engineering Failure Analysis, **80**, 49–56 (2017). https://doi.org/10.1016/j.engfailanal.2017.03.011

[13] Aghdasi A. H., Khonsari M. M.: Friction behavior of radial shaft sealing ring subjected to unsteady motion. Mechanism and Machine Theory, **156**, 104171 (2021). https://doi.org/10.1016/j.mechmachtheory.2020.104171

[14] Ferreira M. J., Almeida M. F., Freitas F.: Formulation and characterization of leather and rubber wastes composites. Polymer Engineering and Science, **51**, 1418–1427 (2011). https://doi.org/10.1002/pen.21643

[15] Bretschger L., Vinogradova A.: Human development at risk: Economic growth with pollution-induced health shocks. Environmental and Resource Economics, **66**, 481–495 (2016). https://doi.org/10.1007/s10640-016-0089-0

[16] Zhang Y., Zhang Z., Wemyss A. M., Wan C., Liu Y., Song P., Wang S.: Effective thermal-oxidative reclamation of waste tire rubbers for producing high-performance rubber composites. ACS Sustainable Chemistry and Engineering, **8**, 9079–9087 (2020). https://doi.org/10.1021/acssuschemeng.0c02292

[17] Thomas B. S., Gupta R. C.: A comprehensive review on the applications of waste tire rubber in cement concrete. Renewable and Sustainable Energy Reviews, **54**, 1323–1333 (2016). https://doi.org/10.1016/j.rser.2015.10.092

[18] Rao B. S., Palanisamy A.: Synthesis of bio based low temperature curable liquid epoxy, benzoxazine monomer system from cardanol: Thermal and viscoelastic properties. European Polymer Journal, **49**, 2365–2376 (2013). https://doi.org/10.1016/j.eurpolymj.2013.05.029

[19] Wang X., Zhou S., Guo W-W., Wang P-L., Xing W., Song L., Hu Y.: Renewable cardanol-based phosphate as a flame retardant toughening agent for epoxy resins. ACS Sustainable Chemistry and Engineering, **5**, 3409–3416 (2017). https://doi.org/10.1021/acssuschemeng.7b00062

[20] Gour R. S., Raut K. G., Badiger M. V.: Flexible epoxy novolac coatings: Use of cardanol-based flexibilizers. Journal of Applied Polymer Science, **134**, 44920 (2017). https://doi.org/10.1002/app.44920

[21] Greco A., Maffezzoli A.: Cardanol derivatives as innovative bio-plasticizers for poly-(lactic acid). Polymer Degradation and Stability, **132**, 213–219 (2016). https://doi.org/10.1016/j.polymdegradstab.2016.02.020

[22] Huang J., Guo W., Wang X., Song L., Hu Y.: Intrinsically flame retardant cardanol-based epoxy monomer for high-performance thermosets. Polymer Degradation and Stability, **186**, 109519 (2021). https://doi.org/10.1016/j.polymdegradstab.2021.109519

[23] Wazarkar K., Sabnis A.: Cardanol based anhydride curing agent for epoxy coatings. Progress in Organic Coatings, **118**, 9–21 (2018). https://doi.org/10.1016/j.porgcoat.2018.01.018

[24] Shishlov O., Dozhdikov S., Glukhikh V., Eltsov O., Kraus E., Orf L., Heilig M., Stoyanov O.: Synthesis of bromo-cardanol novolac resins and evaluation of their effectiveness as flame retardants and adhesives for particleboard. Journal of Applied Polymer Science, **134**, 45322 (2017). https://doi.org/10.1002/app.45322

[25] Je H., Won J.: Natural urushiol as a novel under-water adhesive. Chemical Engineering Journal, **404**, 126424 (2021). https://doi.org/10.1016/j.cej.2020.126424

[26] Wazarkar K., Kathalewar M., Sabnis A.: Anticorrosive and insulating properties of cardanol based anhydride curing agent for epoxy coatings. Reactive and Functional Polymers, **122**, 148–157 (2018). https://doi.org/10.1016/j.reactfunctpolym.2017.11.015

[27] Singaravelu D. L., Vijay R., Filip P.: Influence of various cashew friction dusts on the fade and recovery characteristics of non-asbestos copper free brake friction composites. Wear, **427**, 1129–1141 (2019). https://doi.org/10.1016/j.wear.2018.12.036

[28] Dhanania S., Mahata D., Prabhavale O., Cornish K., Nando G. B., Chattopadhyay S.: Phosphorylated cardanol prepolymer grafted guayule natural rubber: An advantageous green natural rubber. Iranian Polymer Journal, **27**, 307–318 (2018). https://doi.org/10.1007/s13726-018-0611-z

[29] Prabhavale O., Mahata D., Nando G. B.: Phosphorylated cardanol prepolymer-grafted carboxylated styrene-butadiene rubber for better processing with enhancing silica filler dispersion. Journal of Applied Polymer Science, **136**, 47528 (2019). https://doi.org/10.1002/app.47528

[30] Samantarai S., Nag A., Singh N., Dash D., Basak A., Nando G. B., Das N. C.: Cardanol functionalized carboxylated acrylonitrile butadiene rubber for better processability, technical properties and biocompatibility. Journal of Polymers and the Environment, **27**, 1878–1896 (2019). https://doi.org/10.1007/s10924-019-01441-y

[31] Samantarai S., Mahata D., Nag A., Nando G. B., Das N. C.: Functionalization of acrylonitrile butadiene rubber with meta-pentadecenyl phenol, a multifunctional additive and a renewable resource. Rubber Chemistry and Technology, **90**, 683–698 (2017). https://doi.org/10.5254/rct.17.83728

[32] Samantarai S., Nag A., Singh N., Dash D., Basak A., Nando G. B., Das N. C.: Chemical modification of nitrile rubber in the latex stage by functionalizing phosphorylated cardanol prepolymer: A bio-based plasticizer and a renewable resource. Journal of Elastomers and Plastics, **51**, 99–129 (2018). https://doi.org/10.1177/0095244318768644

[33] Mohapatra S., Nando G. B.: Chemical modification of natural rubber in the latex stage by grafting cardanol, a waste from the cashew industry and a renewable resource. Industrial and Engineering Chemistry Research, **52**, 5951–5957 (2013). https://doi.org/10.1021/ie400195v

[34] Mohapatra S., Nando G. B.: Cardanol: A green substitute for aromatic oil as a plasticizer in natural rubber. RSC Advances, **4**, 15406–15418 (2014). https://doi.org/10.1039/c3ra46061d

[35] Mohapatra S., Alex R., Nando G. B.: Cardanol grafted natural rubber: A green substitute to natural rubber for enhancing silica filler dispersion. Journal of Applied Polymer Science, **133**, 43057 (2016). https://doi.org/10.1002/app.43057

[36] Zhang W., Zhang T., Jiang N., Zhang T.: Chemical modification of neoprene rubber by grafting cardanol, a versatile renewable materials from cashew industry. Journal of Polymer Research, **27**, 163 (2020). https://doi.org/10.1007/s10965-020-02122-4

[37] Jacomin A-C., Samavedam S., Charles H., Nezis I. P.: Ilir@viral: A web resource for lir motif-containing proteins in viruses. Autophagy, **13**, 1782–1789 (2017). https://doi.org/10.1080/15548627.2017.1356978

[38] Li H., Zong X., Li N., Zhang X., He A.: Influences of crosslinkable crystalline copolymer on the polymer network and filler dispersion of NR/ESBR/CB nanocomposites. Composites Part A: Applied Science and Manufacturing, **140**, 106194 (2021). https://doi.org/10.1016/j.compositesa.2020.106194